

STUDY ON PREYIELD SHEAR STIFFNESS OF DIFFERENTIAL RESTORING FORCE MODEL FOR LEAD RUBBER BEARING

J.J. JIN¹, F.L. Zhou², P. Tan³, X.Y. Huang⁴, X.Z. Zhuang⁵, C.Y. Shen⁶

¹ Ph.D. student, School of Civil Engineering, Xi'an University of Architecture and Technology, Xi'an, China

¹ Engineer, Earthquake Engineering Research & Test Center, Guangzhou University, Guangzhou, China

² Professor, Earthquake Engineering Research & Test Center, Guangzhou University, Guangzhou, China

³ Professor, Earthquake Engineering Research & Test Center, Guangzhou University, Guangzhou, China

⁴ Associate Professor, Earthquake Engineering Research & Test Center, Guangzhou University, Guangzhou, China

⁵ Associate Professor, Earthquake Engineering Research & Test Center, Guangzhou University, Guangzhou, China

⁶ Associate Professor, Earthquake Engineering Research & Test Center, Guangzhou University, Guangzhou, China

ABSTRACT :

This paper introduces development of differential restoring model (Bouc-Wen model) for lead rubber bearing and its application in seismic-isolation design. At present, SAP2000 and ETABS are used very widely in seismic isolation design. When the preyield shear stiffness of the Bouc-Wen model for LRB is varied, the corresponding hysteretic loop is different. The value and range of the preyield shear stiffness of the Bouc-Wen model for LRB are defined quite different according to seismic isolation codes of different countries. which may result in significant computational errors. Compression-shear tests of two different LRBs are conducted in this paper. The predicted differential restoring force model with various preyield shear stiffness ranging from $5 K_d$ to $40 K_d$ is considered and compared with the experimental results. Some important conclusions can be drawn from the results. An eight-story isolated building is used as the numerical example, in which the preyield shear stiffness of the LRB is chosen $10 K_d$ to $40 K_d$, meanwhile the stiffness of the superstructure is $100 K_d$, $300 K_d$, $500 K_d$ for each shear stiffness of the LRB. Thus the effect of different initial shear stiffness on the structure with various natural periods can be considered and compared. Finally, a reasonable value and range of the preyield shear stiffness of the lead rubber bearing is given in design of the isolated building using commercial program such as SAP2000 or ETABS are given in this paper.

KEYWORDS: lead rubber bearing; differential restoring force model; preyield shear stiffness; compression-shear test

1. DIFFERENTIAL RESTORING FORCE MODEL

The lead rubber isolation bearing (LRB) is constructed by traditional rubber bearing and lead-core which is inserted into the former, the diameter of the lead-core is usually $1/5 \sim 1/7$ times of the outer diameter of the rubber bearing, and the lead has the properties that its yield stress is about 8 kN/mm^2 , having correlation with the deformation velocity and can recover when unloading, dissipating the seismic energy. The lead rubber isolation bearing (LRB) integrates the functions of the rubber bearing and the lead-core. As to far, the lead rubber isolation bearing is the most widely used isolation device^[1].

Bouc proposed the differential equation to describe the smooth hysteresis restoring force in 1976, Wen(1976)^[2], Park et al^[3] generalized this kind of problems and obtained differential equation which can summary the characteristic of a large class of smooth restoring force, and this differential equation can simulate the properties of the restoring force of the LRB.

According to Bouc-Wen model, the properties of the lead rubber isolation bearing are taken into account, the analysis model can be combined by linear force and hysteresis force

$$F = \alpha K_1 D + (1 - \alpha) Q_d z \quad (1.1)$$

where F is restoring force, K_1 is preyield stiffness, α is the ratio of postyield stiffness to preyield stiffness, D is the horizontal shear displacement of the bearing, Q_d is yield load, z is evolutionary variable without

dimension and the range of z is $|z| \leq 1$, which can be obtained from the equations written as follows

$$\dot{z}D_y = A\dot{D} - \gamma|\dot{D}|z|z|^{n-1} - \beta\dot{D}|z|^n \quad (1.2)$$

in which D_y is the yield displacement, the parameters such that A , γ , β decide the shape of hysteresis loop, and those parameters are usually selected $A = 1$, $\gamma = \beta = 0.5$ for lead rubber isolation bearing. Then Eq.(1.2) can be simplified into

$$\dot{z} = \frac{1}{D_y} \begin{cases} \dot{D}(1 - |z|^n) & \dot{D}z > 0 \\ \dot{D} & \text{the others} \end{cases} \quad (1.3)$$

The analysis model of lead rubber isolation bearing can be expressed by bi-directional coupled model

$$\begin{aligned} F_x &= \alpha_x K_{1x} D_x + (1 - \alpha) Q_{dx} z_x \\ F_y &= \alpha_y K_{1y} D_y + (1 - \alpha) Q_{dy} z_y \end{aligned} \quad (1.4)$$

where F_x , F_y is the restoring force of x , y direction, Q_{dx} , Q_{dy} is the yield load of x , y direction, D_x , D_y are the horizontal shear displacements of the bearing in x , y direction, z_x , z_y is the evolutionary variable without dimension which considering bi-directional coupled action and the direction of restoring force, satisfied $\sqrt{z_x^2 + z_y^2} \leq 1$, the summation of initial deformation is zero, and those two variables can be obtained from the equations written as follows

$$\begin{cases} \dot{z}_x D_x^y \\ \dot{z}_y D_y^y \end{cases} = \begin{cases} A\dot{D}_x \\ A\dot{D}_y \end{cases} - \begin{bmatrix} z_x^2 (\gamma \operatorname{sgn}(\dot{D}_x z_x) + \beta) & z_x z_y (\gamma \operatorname{sgn}(\dot{D}_y z_y) + \beta) \\ z_x z_y (\gamma \operatorname{sgn}(\dot{D}_x z_x) + \beta) & z_y^2 (\gamma \operatorname{sgn}(\dot{D}_y z_y) + \beta) \end{bmatrix} \begin{cases} \dot{D}_x \\ \dot{D}_y \end{cases} \quad (1.5)$$

in which D_x^y , D_y^y , \dot{D}_x , \dot{D}_y are horizontal yield displacement and shear deformation velocity of x , y direction respectively.

Set $A = 1$, $\gamma = \beta = 0.5$, then Eq.(1.5) is simplified into^[4]

$$\begin{cases} \dot{z}_x \\ \dot{z}_y \end{cases} = \begin{cases} 1 - \alpha_x z_x^2 & -\alpha_y z_x z_y \\ -\alpha_x z_x z_y & 1 - \alpha_y z_y^2 \end{cases} \begin{cases} \frac{K_x}{Q_{dx}} \dot{D}_x \\ \frac{K_y}{Q_{dy}} \dot{D}_y \end{cases} \quad (1.6)$$

in which $\alpha_x, \alpha_y = \begin{cases} 1 & \dot{D}z > 0 \\ 0 & \text{the others} \end{cases}$

Then Eq.(1.5) has the form of Eq.(1.2), set $n=2$, when $D_x^x = 0$ and $D_y^y = 0$, then this equation turn to represent uniaxial restoring force model.

2. COMPARISONS OF HYSTERESIS LOOP BETWEEN NUMERICAL DIFFERENTIAL MODEL AND COMPRESSION-SHEAR TEST

The most popular finite software used for designing the isolated buiding is SAP2000 and ETABS at present, the theories of the two programs are similar, which are based on bi-directional coupled restoring force model.

In the process of designing, it is easy to determine the characteristic parameters of rubber bearing, but the ratio of the preyield stiffness to postyield stiffness of LRB is difficult to determine, the designer may chose 8 times, 10 times or other values. Those parameters are different according to the material of LRB, construction and various analytical model of isolated building, the international standard “Rubber bearings (PART 3)” suggest this value should be selected as 10-15^[5]. With regard to the effect of various preyield stiffness on the seismic isolation design, quite a few papers have been published, and this is the main research of this paper.

In this paper, the predicted differential restoring model with various ratios of preyield shear stiffness to postyield stiffness (5, 10, 15, 20, 25, 30, 35, 40 times) are taken into account and compared with that of the experimental results. The experimental parameters of LRB are listed in Table 2.1.

The third cycle of hysteresis loop obtained from experimental results of LRB-G4-600-120 and LRB-G4-800-160 together with numerical analysis results using Bouc-Wen model governed by Eq.(1.7) are plotted in Figure 1 and Figure 2. The spring element- post stiffness (K_d) and equivalent stiffness (K_{eq}), damping element- yield force (Q_d) and equivalent damping ratio (H_{eq}), the envelope area of the hysteresis curve (W_d) are listed in Table 2.1-2.2. The post stiffness (K_d) of the experiment and numerical analysis are equal when the deformation is zero, so this parameter is not given in Table 2.2-2.3, and W_d is listed for comparative meaning. The simulation error between the experiment and numerical analysis is described as follows

$$ER = \frac{\sum_{i=1}^n (F_{ii} - F_{mi})^2}{\sum_{i=1}^n F_{ii}^2} \quad (2.1)$$

where F_{ii} and F_{mi} is the restoring force of the i th point obtained from experimental measurement and numerical analysis respectively.

Table 2.1 Data for LRB

| Bearing type | LRB-G4-600-120 | LRB-G4-800-160 |
|---|----------------|----------------|
| Shear modulus of rubber /MPa | 0.392 | |
| Diameter D/mm | 600 | 800 |
| Diameter of lead Dp/ mm | 120 | 160 |
| Total height of inner rubber/mm | 120 | 160 |
| S1 | 37.5 | 40 |
| S2 | 5 | 5 |
| Postyield stiffness/ (kN·m ⁻¹) | 929 (918) | 1239 (1274) |
| Yield force/kN | 90.2 (94.47) | 160.3 (160.6) |
| Horizontal stiffness($\gamma=100\%$)/ (kN·m ⁻¹) | 1681 (1550) | 2241 (2087) |
| Equivalent damping ratio | 0.265 (0.307) | 0.265 (0.298) |

The values of the experimental measurement are offered in brackets.

From the comparison results we can find that:

- (1) The error index, ER, is bigger than 9% the preyield stiffness is 5 and 10 times of postyield stiffness. The error index is closed to 5% when choosing 15 times, and it becomes smaller when the times is bigger. In the mean while, the larger the times, the smaller the ER, and this conclusion is obtained only from the unloading stiffness.
- (2) When the times is larger than 15, H_{eq} and W_d are superior to those of less than 10.
- (3) As for the 10 and 15 times cases, not only every performance indexes, but also the unloading stiffness, the

latter is perform better than the former

Table 2.2 Performance indexes comparison of LRB-G4-600-120

| Index | Test result | 5 | 10 | 15 | 20 | 25 | 30 | 35 | 40 |
|-----------------|-------------|------------------|------------------|------------------|------------------|------------------|-------------------|-------------------|-------------------|
| K_{eq} (kN/m) | 1500 | 1699 (109.6%) | 1699 (109.6%) | 1699 (109.6%) | 1699 (109.6%) | 1699 (109.6%) | 1699 (109.6%) | 1699 (109.6%) | 1699 (109.6%) |
| H_{eq} | 0.307 | 0.219 (71.3%) | 0.258 (84.3%) | 0.270 (88.0%) | 0.275 (89.7%) | 0.278 (90.8%) | 0.280 (91.4%) | 0.282 (91.9%) | 0.283 (92.2%) |
| W_d (N*m) | 43777 | 34247 (78.2%) | 40444 (92.4%) | 42225 (96.5%) | 43070 (98.4%) | 43563 (99.5%) | 43884 (100.2%) | 44107 (100.8%) | 44266 (101.1%) |
| ER (%) | | 20.4% | 9.3% | 5.9% | 4.2% | 3.4% | 3.0% | 2.7% | 2.6% |

The ratio values of the numerical simulation and experimental results are offered in brackets.

Table 2.3 Performance indexes comparison of LRB-G4-800-160

| Index | Test result | 5 | 10 | 15 | 20 | 25 | 30 | 35 | 40 |
|-----------------|-------------|------------------|------------------|------------------|------------------|------------------|------------------|-------------------|-------------------|
| K_{eq} (kN/m) | 2087 | 2292 (109.8%) | 2292 (109.8%) |
| H_{eq} | 0.298 | 0.216 (72.5%) | 0.252 (84.4%) | 0.262 (87.8%) | 0.267 (89.4%) | 0.270 (90.4%) | 0.272 (91.0%) | 0.273 (91.5%) | 0.274 (91.8%) |
| W_d (N*m) | 97108 | 77349 (79.7%) | 89999 (92.7%) | 93645 (96.4%) | 95388 (98.2%) | 96420 (99.3%) | 97096 (99.9%) | 97564 (100.5%) | 97901 (100.8%) |
| ER (%) | | 17.6% | 9.2% | 6.6% | 5.3% | 4.5% | 4.0% | 3.7% | 3.5% |

The ratio values of the numerical simulation and experimental results are offered in brackets.

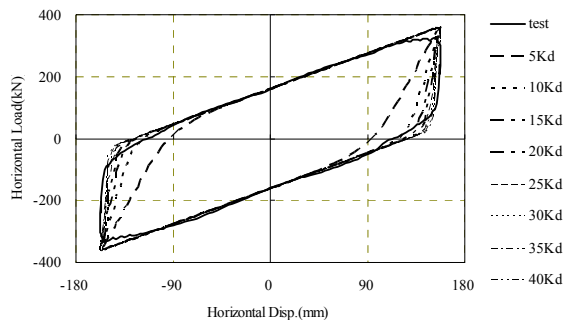


Figure 1 Hysteresis curve of LRB-G4-600-120 obtained from experiment and simulation

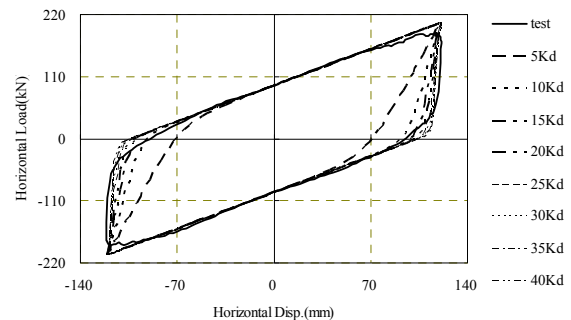


Figure 2 Hysteresis curve of LRB-G4-800-160 obtained from experiment and simulation

3. COMPUTATIONS OF ISOLATION BUILDING WITH DIFFERENT PARAMETERS

Based on the conclusions of the former sections, an 8-story base isolated building using Bouc-Wen model with different preyield stiffness is simulated. The parameters of this structure is listed in Table 3.1, the isolation bearing is selected as LRB-G4-800-160. The stiffness of the first floor of superstructure is chosen as 100, 300, 500 times of the post stiffness of the bearing, the stiffness of the top floor is set to 0.5 times that of the first floor, and the stiffnesses of the other floors are determined by interpolating. The first period is 0.826s, 0.477s and 0.369s when the base is fixed, respectively. When the stiffness of the isolation layer is equal to preyield stiffness (set $K_1 = 15K_d$), the first period is 1.311s, 1.155s and 1.124s, respectively; When the stiffness of the isolation layer is equal to postyield stiffness, the first period is 4.229s, 4.188s and 4.180s, respectively.

Table 3-1 Data of simulated model

| Floor | Mass (t) | Horizontal stiffness(kN/mm) | | |
|-------------------------------|----------------------------------|-----------------------------|-----------|-----------|
| | | $100 k_d$ | $300 k_d$ | $500 k_d$ |
| 9 | 60.582 | 61.95 | 185.85 | 309.75 |
| 8 | 60.582 | 70.80 | 212.40 | 354.00 |
| 7 | 60.582 | 79.65 | 238.95 | 398.25 |
| 6 | 60.582 | 88.50 | 265.50 | 442.50 |
| 5 | 60.582 | 97.35 | 292.05 | 486.75 |
| 4 | 60.582 | 106.20 | 318.60 | 531.00 |
| 3 | 60.582 | 115.05 | 345.15 | 575.25 |
| 2 | 60.582 | 123.90 | 371.70 | 619.50 |
| 1 (isolation layer) | 60.582 | | | |
| Total mass/(t) | 545.24 | | | |
| Parameter for isolation layer | Yield force /(kN) | 160.3 | | |
| | Postyield stiffness(kN/mm) | 1.239 | | |
| | Shear coefficient at yield point | 0.03 | | |

Artificial waves for frequent earthquake and rare earthquake (earthquake intensity VIII) based on Chinese design response spectrum are employed as external input, the peak acceleration is 0.71m/s^2 and 3.87m/s^2 respectively. The preyield stiffness is 10, 15, 20, 25, 30, 35, 40 times of the postyield stiffness, and the viscous damping of the isolation layer is not take into account, the equivalent damping ratio is 5%.

Table 3.2 (subjected to frequent earthquake, $100 K_d$) and Figure 3 present the responses of acceleration with different stiffness ratio, it is observed that acceleration is linear distribution with turning point of the middle floor, and there is a increasing trend of acceleration of upper floors but this trend decreases when the superstructure becomes rigid. This change is relatively greater when the ratio of the preyield stiffness to postyield stiffness is chosen as 10 and 15.

Table 3.3 shows the peak relative displacement of isolation layer, it is observed that the peak displacement of isolation layer decrease with the increment of the preyield stiffness of the bearing.

Table 3.4 (subjected to frequent earthquake, $100 K_d$) and Figure 4 show the peak interstory drift of each floor with different stiffness ratio, the change of the peak interstory drift is relatively larger when the ratio of the preyield stiffness to postyield stiffness is chosen as 10 and 15.

Table 3.5 (subjected to frequent earthquake, $100 K_d$) and Figure 5 show the shear coefficient with different stiffness ratio, it is observed that the shear coefficient increase with the increment of the preyield stiffness of the bearing. When subjected to frequent earthquakes ($100 K_d$), the change of the shear coefficient is relatively larger when the ratio of the preyield stiffness to postyield stiffness is chosen as 10 and 15. According to the Chinese code, the design is usually based on the shear coefficient, and the shear force of the floors above the interlayer will be underestimated.

Table 3.2 Peak acceleration response(m/s^2)

| Floor | Preyield stiffness/postyield stiffness | | | | | | |
|-------|--|-------|-------|-------|-------|-------|-------|
| | 10 | 15 | 20 | 25 | 30 | 35 | 40 |
| 9 | 0.474 | 0.620 | 0.701 | 0.718 | 0.768 | 0.789 | 0.809 |
| 8 | 0.433 | 0.553 | 0.617 | 0.607 | 0.649 | 0.673 | 0.688 |
| 7 | 0.379 | 0.454 | 0.491 | 0.470 | 0.483 | 0.502 | 0.514 |
| 6 | 0.334 | 0.371 | 0.373 | 0.380 | 0.405 | 0.411 | 0.405 |
| 5 | 0.341 | 0.358 | 0.361 | 0.390 | 0.392 | 0.420 | 0.445 |
| 4 | 0.369 | 0.414 | 0.435 | 0.414 | 0.435 | 0.462 | 0.482 |
| 3 | 0.389 | 0.457 | 0.495 | 0.470 | 0.483 | 0.500 | 0.516 |
| 2 | 0.399 | 0.482 | 0.533 | 0.506 | 0.478 | 0.485 | 0.483 |
| 1 | 0.399 | 0.490 | 0.545 | 0.519 | 0.485 | 0.463 | 0.451 |

Table 3.3 Peak relative displacement of isolation layer(mm)

| | Preyield stiffness/postyield stiffness | | | | | | |
|-------------------------------|--|-------|-------|-------|-------|-------|-------|
| | 10 | 15 | 20 | 25 | 30 | 35 | 40 |
| frequent earthquake、 $100k_d$ | 23.0 | 21.9 | 20.6 | 15.4 | 13.5 | 13.8 | 13.7 |
| frequent earthquake、 $300k_d$ | 24.3 | 21.5 | 15.1 | 13.3 | 13.7 | 14.2 | 14.2 |
| frequent earthquake、 $500k_d$ | 25.3 | 20.4 | 15.0 | 14.7 | 14.7 | 13.8 | 12.5 |
| rare earthquake、 $100k_d$ | 338.1 | 337.0 | 330.9 | 332.1 | 333.0 | 334.5 | 336.2 |
| rare earthquake、 $300k_d$ | 331.6 | 324.2 | 328.3 | 328.0 | 327.6 | 329.7 | 331.8 |
| rare earthquake、 $500k_d$ | 330.6 | 324.6 | 328.0 | 327.0 | 328.7 | 331.0 | 332.3 |

Table 3.4 Peak interstory drift(mm)

| Floor | Preyield stiffness/postyield stiffness | | | | | | |
|-------|--|-------|-------|-------|-------|-------|-------|
| | 10 | 15 | 20 | 25 | 30 | 35 | 40 |
| 9 | 0.46 | 0.60 | 0.68 | 0.69 | 0.74 | 0.77 | 0.78 |
| 8 | 0.77 | 1.00 | 1.12 | 1.12 | 1.19 | 1.24 | 1.26 |
| 7 | 0.97 | 1.23 | 1.37 | 1.34 | 1.43 | 1.48 | 1.51 |
| 6 | 1.09 | 1.34 | 1.48 | 1.41 | 1.50 | 1.56 | 1.60 |
| 5 | 1.15 | 1.38 | 1.49 | 1.42 | 1.49 | 1.54 | 1.58 |
| 4 | 1.18 | 1.38 | 1.46 | 1.39 | 1.41 | 1.47 | 1.50 |
| 3 | 1.19 | 1.35 | 1.41 | 1.35 | 1.32 | 1.37 | 1.40 |
| 2 | 1.24 | 1.32 | 1.35 | 1.30 | 1.27 | 1.28 | 1.29 |
| 1 | 23.05 | 21.93 | 20.55 | 15.37 | 13.49 | 13.80 | 13.70 |

Table 3.5 shear coefficient

| Floor | Preyield stiffness/postyield stiffness | | | | | | |
|-------|--|-------|-------|-------|-------|-------|-------|
| | 10 | 15 | 20 | 25 | 30 | 35 | 40 |
| 9 | 0.048 | 0.063 | 0.072 | 0.073 | 0.078 | 0.081 | 0.083 |
| 8 | 0.046 | 0.060 | 0.067 | 0.068 | 0.072 | 0.075 | 0.076 |
| 7 | 0.044 | 0.055 | 0.061 | 0.060 | 0.065 | 0.067 | 0.068 |
| 6 | 0.041 | 0.050 | 0.055 | 0.053 | 0.057 | 0.059 | 0.060 |
| 5 | 0.038 | 0.046 | 0.049 | 0.047 | 0.049 | 0.051 | 0.052 |
| 4 | 0.035 | 0.041 | 0.044 | 0.042 | 0.042 | 0.044 | 0.045 |
| 3 | 0.033 | 0.037 | 0.039 | 0.037 | 0.037 | 0.038 | 0.039 |
| 2 | 0.032 | 0.034 | 0.035 | 0.034 | 0.033 | 0.033 | 0.034 |
| 1 | 0.033 | 0.035 | 0.035 | 0.034 | 0.033 | 0.033 | 0.033 |

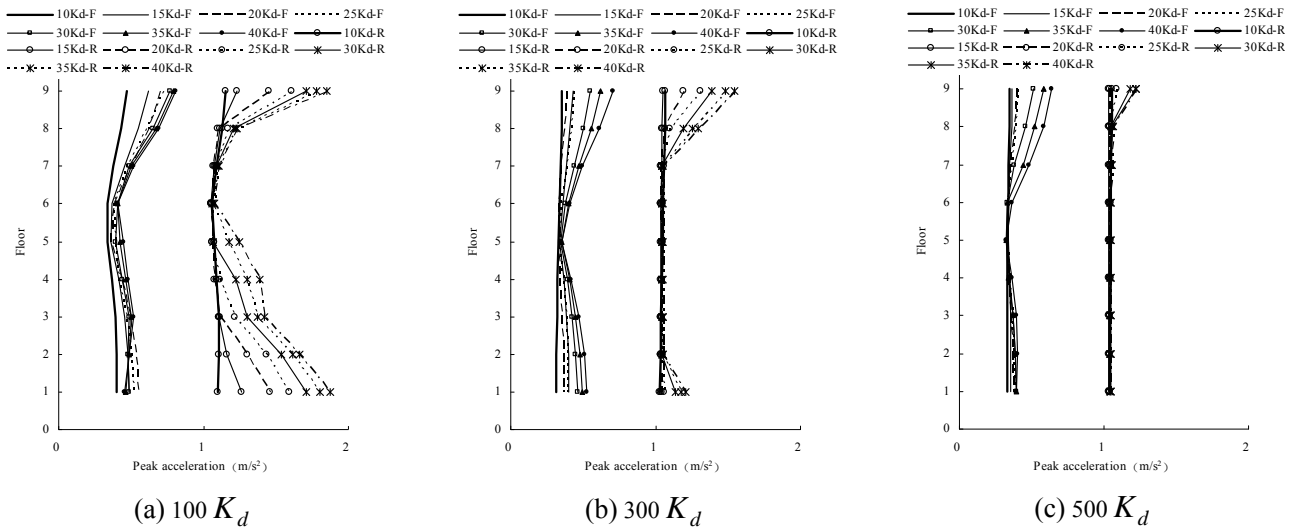


Figure 3 Peak accelerations response

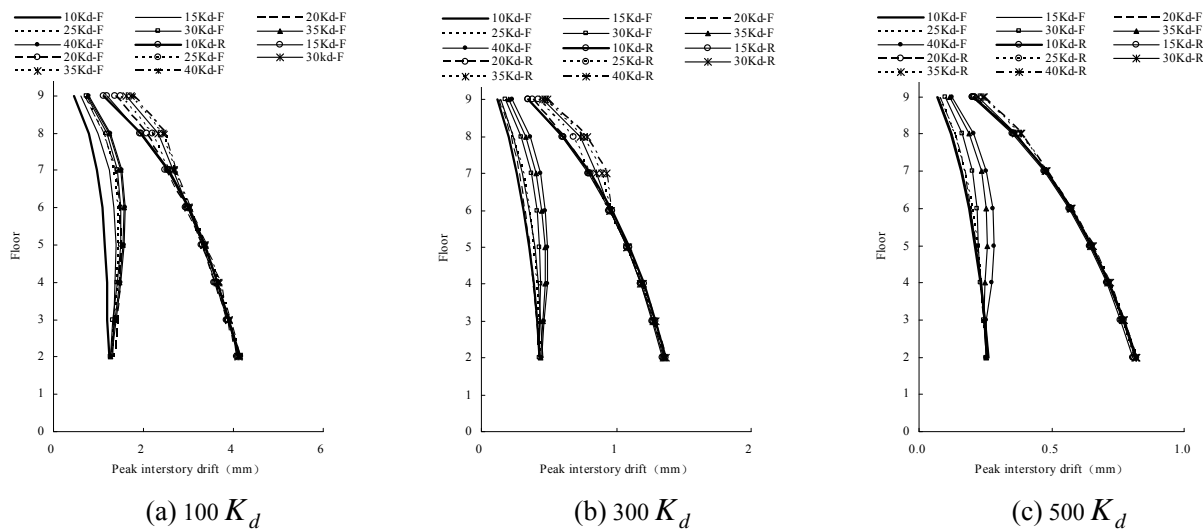


Figure 4 Peak interdrift displacement

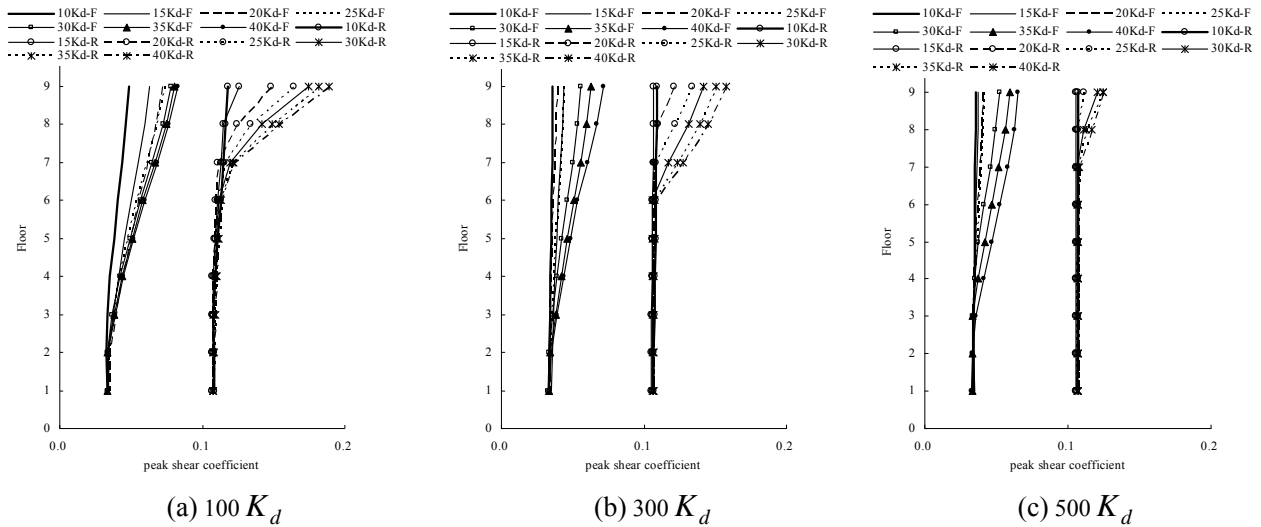


Figure 5 Peak shear coefficient

In figure 3,4,5 ,F is frequent earthquake ,R is rare earthquake.

4.CONCLUSIONS

The reasonable value of preyield stiffness for seismic isolation design has been investigated. Some useful conclusions are drawn as follows

- (1) By comparing the hysteresis loop of numerical simulation using Bouc-Wen model with that of the experimental results and the analysis results of isolation structure, the numerical model can not represent the real experimental results when the preyield stiffness is equal to $10 K_d$, but it performs well when the preyield stiffness is larger than $15 K_d$.
- (2) The responses of the superstructure will be underestimated when the preyield stiffness is equal to $10 K_d$, it is observed that the responses of the top layer increase with the increment of the preyield stiffness of the bearing.
- (3) The results of $15 K_d$ is superior to those of $10 K_d$ when designing isolated building using SAP2000 or ETABS, this superiority is obvious when the horizontal stiffness of superstructure is smaller and subjected to frequent earthquake.

From the conclusions above, the reasonable value of preyield stiffness of LRB is suggested to be chosen as $15 K_d$ or larger when using SAP2000 or ETABS to design isolated building.

REFERENCE

- Zhou, F.L. (1997). Seismic control of structures. *Seismological Press*
- Wen, Y.K. (1976). Method for random vibration of hysteretic system. *Journal of the Engineering Mechanics Division* **102**, 249-263.
- Park, Y.J., Wen, Y.K. and Ang, A.H. (1986). Random vibration of hysteretic systems under bi-directional ground motions. *Earthquake Engineering and Structural Dynamics* **14**, 543-557.
- Civil King Software Technology Co.Ltd (2006) . Guide of SAP2000-Chinese version. Beijing: People's communication Press.
- ISO 22762-3:2005 Part 3, Elastomeric seismic-protection isolatorS-Part3: Application for buildings